Journal of Basrah Researches (Sciences) **51**(2), 284 (2025)
DOI: https://doi.org/10.56714/bjrs.51.2.20

Model Calculation for the Chemisorption of Li and Na Atoms on Bilayer Graphene

Batool M. Ajer, Abadhar R. Ahmed*

Physics Department, College of Education for Pure Science, Basrah University, Basrah, Iraq .

ARTICLE INFO

Received 21 October 2025
Revised 13 December 2025
Accepted 22 December 2025
Published 31 December 2025

Keywords:

Bilayer Graphene, Chemisorption, Anderson-Newns Model.

Citation: B. M. Ajer , A. R. Ahmed. , J. Basrah Res. (Sci.) **50**(2), 284 (2025). DOI:https://doi.org/10.56714/bjrs.51.2.20

ABSTRACT

The Anderson-Newns model is used to study the chemisorption process of lithium and sodium atoms on bilayer graphene. The density of states of bilayer graphene is employed, along with the effects of quantum coupling represented by broadening and quantum shift to calculate the electronic properties, magnetization and chemisorption energy. The self-consistent solutions of the atomic occupation numbers revealed that the solution is magnetic at relatively large distances from bilayer graphene, and turn into non-magnetic one at certain close distance. The relationship between the magnetization of atoms and their distance from bilayer plane can be exploited in spintronics applications. Moreover, the ionic contribution to the chemisorption energy dominates at closest approach distances, providing a clear description of the bonding nature with bilayer graphene. These results can take advantage for experimental applications in storage of null magnetization atoms on two dimensional materials.

1. Introduction

Bilayer graphene consists of two layers of graphene stacked together. Each graphene layer is a single sheet of carbon atoms arranged in a hexagonal lattice. When these two layers are placed on top of each other, they form bilayer graphene, which has some unique properties as compared to monolayer graphene [1,2]. Many of the properties of bilayer graphene are similar to those in monolayer [3], such as high electrical conductivity with room temperature mobility up to 40.000 cm2 V-1 S-1 in air [4]; electrical properties can be tuned by doping or changing the carrier density through gating [5]; additionally, high thermal conductivity at room temperature (about 2,800Wm−1K−1)[6]; strength flexibility and mechanical stiffness (Young's modulus is about 0.8 TPa) [7]; transmittance of white light of about 95% with transparency ; impermeability to gases [8]. Therefore, bilayer graphene will possess potential for multiple applications in various fields, such as flexible and transparent electrodes for touch screens, thermoelectric devices, high-frequency transistors, photodetectors, photonic devices, and batteries [9].

The bilayer graphene gap can be tuned through chemical modification from zero up to values typical for conventional semiconductors like silicon or GaAs[10]. In transistors made of graphene, the junction does not close, and this problem is solved by using bilayer graphene because there is a real gap in it [10-13]. Bilayer graphene can be formed by stacking two graphene sheets, rotating one relative to the other. Depending on the twisting angle, this material exhibits magnetic properties, superconductivity, and various other electronic phenomena [14-17]. Some researchers have

***Corresponding author email:** abadhar.ahmed@uobasrah.edu.iq.

ISSN: 1817-2695 (Print); 2411-524X (Online)
Online at: https://jou.jobrs.edu.iq

developed an alternative technique to control the electrons of bilayer graphene. This technique involves sliding one sheet over the other without rotation[18].
One of great significance in practical applications is the variation in the chemical binding energy at the closest point of atom adsorption on bilayer graphene especially in fields that rely on precise control of the electronic and physical properties of nanomaterials. As the distance between the atom and the bilayer graphene changes, the nature of bonding (metallic, ionic, covalent) also changes, affecting the magnetic state of the atom. This is useful in designing tunable magnetic materials. Changes in binding energy affect the distribution of charge carriers in bilayer graphene, allowing for adjustments in electrical conductivity or the opening of a band gap in a semiconducting material. In applications such as hydrogen storage or gas adsorption, controlling the binding energy determines how strongly atoms or molecules attach to bilayer graphene, thereby influencing storage or separation efficiency. Binding energy variation enhances bilayer graphene's ability to efficiently retain hydrogen, tunes electronic properties through adsorption control, increases bilayer graphene's sensitivity to target substances, selects effective adsorption sites to improve reactions, and enables spin control via binding energy for advanced devices. The electronic coupling between layers creates a denser electronic environment, enhancing bonding between the atom and bilayer graphene surface. The Van der Waals interaction between layers stabilizes the adsorbed atom and reduces thermal vibrations. There are multiple adsorption sites in bilayer graphene, atoms can adsorb between layers or on the top surface, offering diverse energetic configurations. Bilayer graphene provides higher binding energy for lithium atoms, increasing storage density in Lithium batteries. Stronger adsorption in bilayer graphene leads to more stable and accurate sensing in chemical sensors. Adsorbed atoms are more stable, improving catalytic performance in chemical reactions for nanocatalysis. Changes in binding energy affect local magnetism, enabling the design of spin-based electronic devices[19-21].
In this work, the chemisorption of atoms on bilayer graphene is studied and investigated using Anderson model to calculate occupation numbers, magnetization and chemical energy for Li and Na atoms adsorbed on bilayer graphene.

2. The Theoretical Treatment

In this study, the Hamiltonian model used of the combined system (adatom/bilayer graphene) is given by [22-24] :

$$H = \sum_{k\sigma} E_k^\sigma n_k^\sigma + \sum_\sigma E_A^\sigma n_A^\sigma + U n_A^\sigma n_A^{-\sigma} + \sum_{k\sigma}(V_{Ak}^\sigma C_A^{\sigma\dagger} C_k^\sigma + V_{kA}^\sigma C_k^{\sigma\dagger} C_A^\sigma) \quad (1)$$

where, E_k^σ and n_k^σ are the energy levels and the corresponding occupation numbers in the bilayer graphene energy band with set of quantum numbers k and spin σ, respectively. E_A^σ is the adsorbed atom spin dependent energy level and n_A^σ is the corresponding occupation number. $C_i^{\sigma\dagger}(C_i^\sigma)$ is the creation (inhalation) operators for the state level $i(=k, A)$ for spin σ. V_{Ak} are the coupling interaction matrix elements. $U(=V_i - V_A)$ is the correlation energy. By taking the image effect and correlation into consideration, the adatom energy level E_A^σ ($E_A^{-\sigma}$) with spin up (spin down) be [25,26]; $E_A^{\pm\sigma}(Z) = E_A^0 + \Delta E(Z) + U_{eff} n_A^{\mp\sigma}$, $E_A^0$is the atom ionization energy with respect to the system energy reference.
The effective correlation energy can be calculated as a function of the normal distance (Z) between adatom and bilayer graphene; $U_{eff}(Z) = V_i - V_A - 2\Delta E(Z)$ [27] with, $\Delta E(Z)(= \frac{e^2/4}{Z+Z_0})$ is the image shift which takes the image effect into consideration[27]; Z_0 represents the closest approach.
The occupation number of the adatom energy level of spin σ $(i.e. E_A^\sigma)$ is given by:

$$n_A^\sigma = \int \quad f(E,T)\rho_{Ad}^\sigma(E)dE \quad (2)$$

ρ_{Ad}^σ is the local density of states on the adatom (which will be highlighted extendedly) and $f(E,T)$ is Fermi distribution function.
The local density of states associated with each atomic level of spin σ is a Lorentzian distribution centered at E_A^σ[23]:

$$\rho_{Ad}^\sigma(E) = \frac{1}{\pi}\frac{\Delta(E)}{[E - E_A^\sigma - \Lambda(E)]^2 + [\Delta(E)]^2} \quad (3)$$

where $\Delta(E)(=\pi|V_0|^2\rho_{BLG}(E))$ and $\Lambda(E)(=\frac{1}{\pi}P\int d\acute{E}\frac{\Delta(\acute{E})}{E-\acute{E}})$ are the energy dependent broadening and quantum shift in the adatom energy level due to coupling interaction between the adsorbate atom and the bilayer graphene. $\rho_{BLG}(E)$ is the bilayer graphene density of states, and V_0 is the strength of the coupling interaction. The density of states for the bilayer graphene is[28]:

$$\rho_{BLG}(E)=\frac{g_s g_v}{2\pi(\hbar v_F)^2}(|E|+\frac{\gamma_1}{2}) \quad (4)$$

where $g_s\ and\ g_v$ represents the spin and valley degeneracy. v_F is the Fermi velocity and γ_1 is the interlayer coupling for bilayer graphene (= 0.39 eV).

The bond that formed between adatom and the bilayer graphene can be divided into an ionic part and metallic part. The expression for the metallic part of the chemisorption energy is given by [25],

$$E_m(Z)=\sum_\sigma\int_{u_\circ}^{\varphi} Ef(E,T)\rho_{Ad}^{\sigma}(E)dE-U_{eff}n_A^{\sigma}n_A^{-\sigma} \quad (5)$$

$u_\circ$is the energy band bottom and φ is the bilayer graphene work function.

The initial state (at $Z=\infty$) is an atom and bilayer graphene separated by "infinite" distance, so we write,

$$E_m(\infty)=\sum_\sigma\int_{u_\circ}^{\varphi} Ef(E,T)\delta(E-E_A^0)dE \quad (6)$$

Which, we write [26]

$$\begin{aligned}E_m(\infty)&=E_A^{\circ}f(E_A^0,T)\\&=(\varphi-V_i)\Theta(V_i-\varphi)\end{aligned} \quad (7)$$

With Θ is unit step function. Now, the chemisorption energy can be calculated by using the following relation,

$$E_{ch}(Z)=E_m(Z)+E_{ion}(Z) \quad (8)$$

$E_{ion}(Z)$ is the ionic part of the chemisorption energy and given by[25];

$$E_{ion}(Z)=-e^2\int_Z^\infty\frac{Z_{eff}^2(Z')}{4(Z+Z_\circ)^2}dZ' \quad (9)$$

The effective charge number of the atom $Z_{eff}(Z)$ is a function of distance;

$$Z_{eff}(Z)=1-n_A^{\sigma}(Z)-n_A^{-\sigma}(Z) \quad (10)$$

3. Results

In order to achieve all the calculations, the equations concerned to $E_A^{\sigma}(Z)$ and $n_A^{\sigma}(Z)$ are solved self-consistently. By using the impurity Anderson model, all functions that describe the chemisorption process for any atom on bilayer graphene can be included in the self-consistent solution which is numerically accomplished. All parameters concerned to the electronic properties of the system that used in our calculations are presented in table(1). V_i (V_A) represents the atom ionization energy (affinity energy), V_0 is the strength of hybridization and Z_0 is the closest approach, while the temperature is fixed at 300K.

Li (Na) atom adsorbed to carbon atom directly, normal to the bilayer graphene plane, in an on top site, i.e. the Li (Na) atom is placed at Z_0 =0.162nm (=0.222 nm) directly above the bilayer graphene. Figure (1) shows the density of states for Bilayer graphene according to the equation (4), this figure confirms the liner relation of the density of states of bilayer graphene vs energy with obvious shift at E=0. One of the first physical features that confirms the correct self-consistent solution is the occupation numbers and the corresponding adsorbed atom energy levels. Figure (2) indicates that the physical solution for the atom adsorbed on bilayer graphene is magnetic solution for all Z values relatively far from the bilayer graphene, then the solution turns to a non-magnetic solution at a certain distance. This distance corresponds to Z=0.502nm in the case of lithium atom, while it corresponds to Z=0.792nm in the case of sodium atom.

These results are also illustrated in Figure (3), where $E_A^{\sigma}(Z)$ is lower than $E_A^{-\sigma}(Z)$ and then become equal and lesser than the mentioned Z values due to the correlation energy and image shift effects.

In order to study the magnetic behavior of lithium and sodium atom adsorbed to bilayer graphene, the magnetization must be calculated ($M=n_A^{\sigma}-n_A^{-\sigma}$) (see Figure (4)). The self-consistent solution shows that the solution is magnetic at Z values relatively far from bilayer graphene, and then it turns to a non-magnetic solution at (Z=0.502 nm) for the case of Li atom and (Z=0.792 nm) for Na atom.

Figure (5) illustrates the chemisorption energy contributions and the total chemisorption energy when atom is attached to bilayer graphene. In the case of Li atom, the ionic energy vanishes at far distances while the metallic energy appears weak. At a certain distance (Z=0.622 nm) the metallic energy vanishes while the ionic energy dominates. In the case of Na atom, the ionic energy vanishes at far distances while the metallic energy appears weak. At a certain distance (Z=1.082 nm) the metallic energy vanishes while the ionic energy dominates.

Table 1. The atom/bilayer graphene system parameters.

Atom	V_i (eV)	V_A (eV)	V_0 (eV)	Z_0 (nm)
Li	5.39	0.62	0.5	0.162
Na	5.14	0.55	0.5	0.222

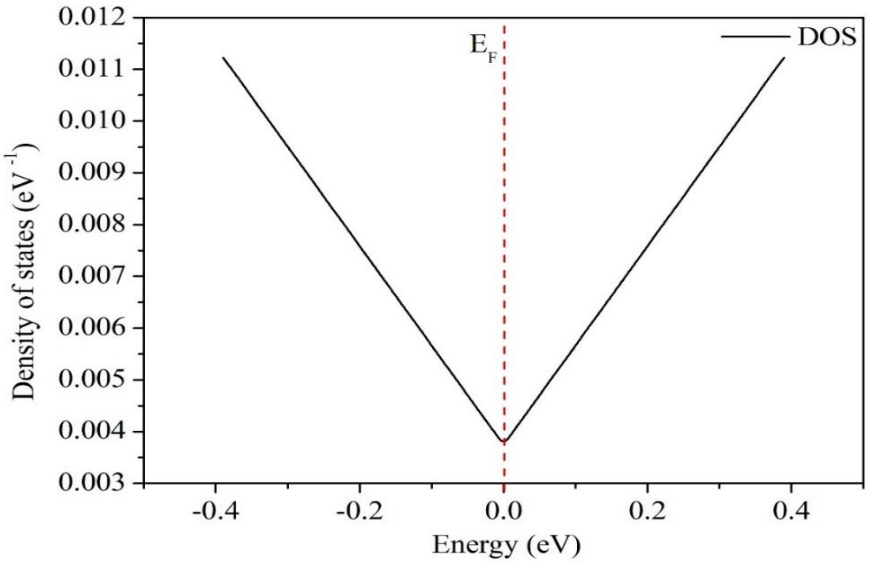

Fig. 1. The Bilayer Graphene density of states.

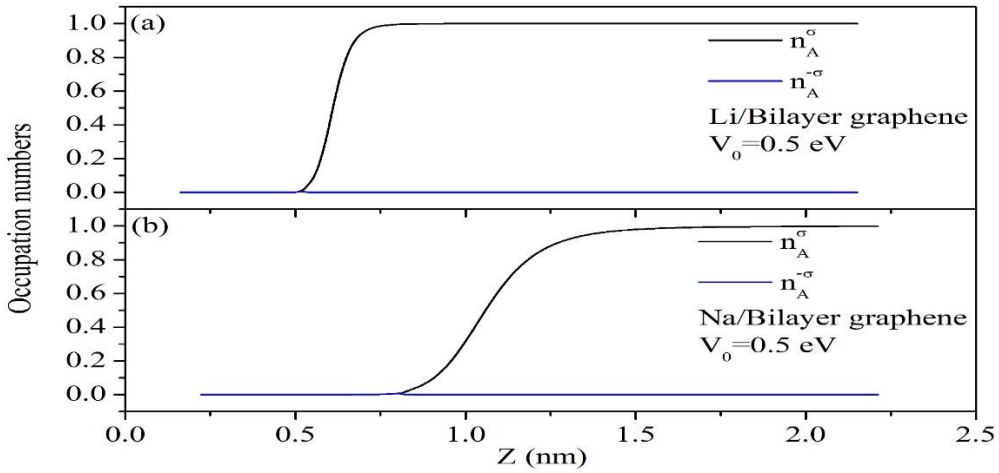

Fig. 2. The occupation numbers as a function of distance for (a) Li/Bilayer Graphene and (b) Na/Bilayer Graphene.

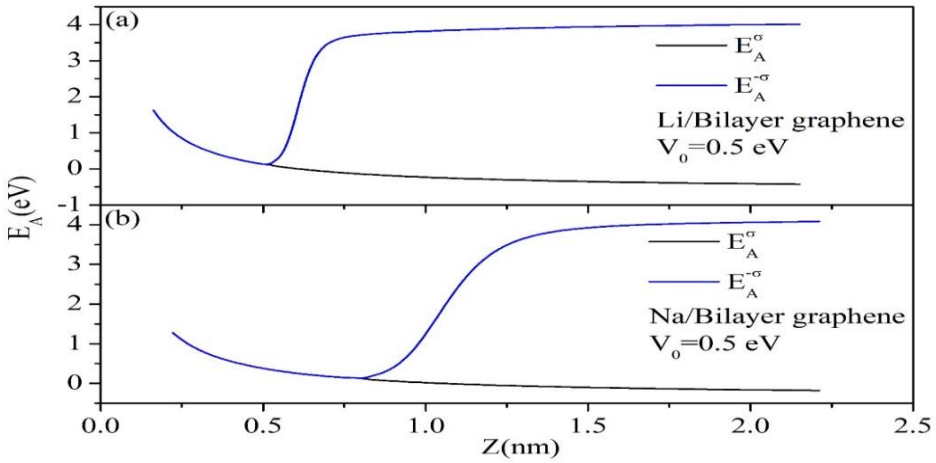

Fig. 3. The adatom energy levels as a function of distance for (a) Li/Bilayer Graphene and (b) Na/Bilayer Graphene.

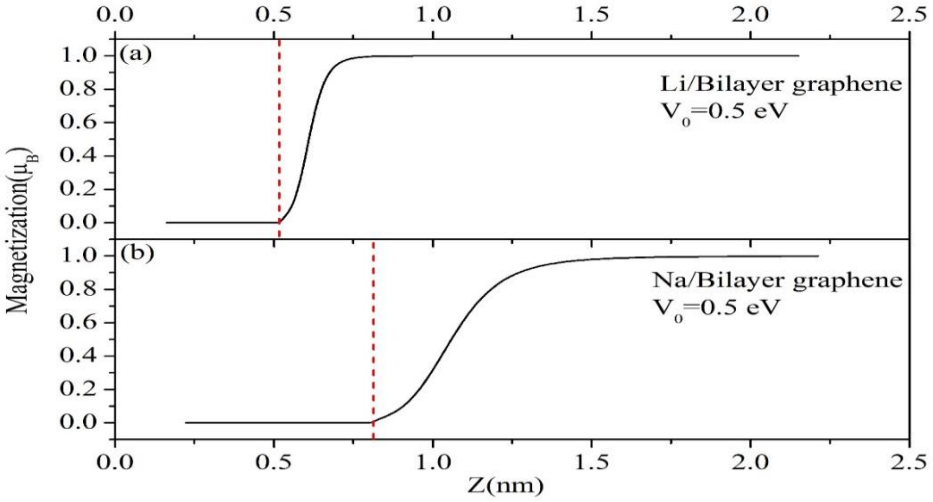

Fig. 4. The magnetization on the adatom as a function of distance for (a) Li/Bilayer Graphene and (b) Na/Bilayer Graphene.

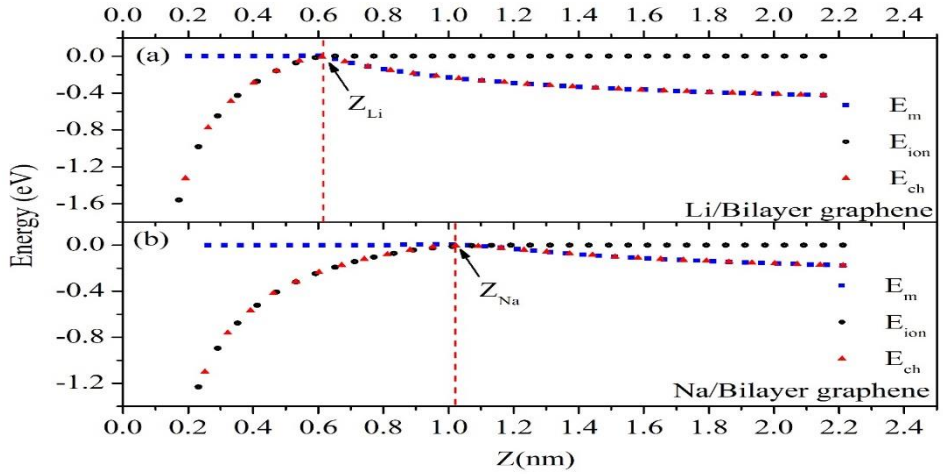

Fig. 5. The chemisorption energy as a function of distance for (a) Li/Bilayer Graphene and (b) Na/Bilayer Graphene.

4. Conclusions

The chemisorption of atoms (molecular or nanoparticles) on bilayer graphene is driven by it's remarkable potential to modulate electronic, magnetic and chemical properties, thereby enabling advanced applications in energy storage, sensing technologies and nanoelectronics. Owing to the presence of interlayer interactions, bilayer graphene provides greater tunability compared to its monolayer counterpart, establishing it as a versatile and promising platform for functionalization and material design. These practical applications motivate the theoretical studies to investigate all the physical properties that can develop these applications.

According to our calculations, interested features can be reported;

1.For values $Z < Z_{Li}$ ($Z < Z_{Na}$), the ground state of the system has ionic energy, while when $Z > Z_{Li}$ ($Z > Z_{Na}$) the ground state of the system is metallic, here, Z_{Li} and Z_{Na} represent the values of Z at which the ionic and metallic energies are equal (see Fig.(5)).

2.The distance at which ionic and metallic energy are equal for Li (Na) atom is 0.622nm (1.082nm). This location is determined by the ionization energy of the atom V_i and the coupling interaction V_0.

3.At closest approach, the chemisorption energy of Li/bilayer graphene be greater than that of Na/bilayer graphene, so this feature can be invested in applications of atoms storage on two dimensional materials.

Finally, the perfect Bilayer Graphene density of states was included in our calculation. However, another formulism, will be presented in the next future work for the deformed Bilayer Graphene which is useful for investigating the mechanical properties of the system under consideration.

References

[1] I. J. Vera-Marun, V. Ranjan, and B. J. van Wees, "Nonlinear detection of spin currents in graphene with non-magnetic electrodes," *Nature Physics*, vol. 8, pp. 313–316, 2012, doi: 10.1038/NPHYS2219.

[2] J. F. Sierra, I. Neumann, J. Cuppens, B. Raes, M. V. Costache, and S. O. Valenzuela, "Thermoelectric spin voltage in graphene," *Nature Nanotechnology*, vol. 13, pp. 107–111, 2018, doi: 10.1038/s41565-017-0015-9.

[3] K. S. Novoselov, V. I. Fal'ko, L. Colombo, P. R. Gellert, M. G. Schwab, and K. Kim, "A roadmap for graphene," *Nature*, vol. 490, pp. 192–200, 2012, doi: 10.1038/nature11458.

[4] C. R. Dean, A. F. Young, I. Meric, C. Lee, L. Wang, S. Sorgenfrei, K. Watanabe, T. Taniguchi, P. Kim, K. L. Shepard, and J. Hone, "Boron nitride substrates for high-quality graphene electronics," *Nature Nanotechnology*, vol. 5, pp. 722–726, 2010, doi: 10.1038/nnano.2010.172.

[5] K. S. Novoselov, E. McCann, S. V. Morozov, V. I. Fal'ko, M. I. Katsnelson, U. Zeitler, D. Jiang, F. Schedin, and A. K. Geim, "Unconventional quantum Hall effect and Berry's phase of 2π in bilayer graphene," *Nature Physics*, vol. 2, pp. 177–180, 2006, doi: 10.1038/nphys245.

[6] A. A. Balandin, "Thermal properties of graphene and nanostructured carbon materials," *Nature Materials*, vol. 10, pp. 569–581, 2011, doi: 10.1038/nmat3064.

[7] Y. Y. Zhang, C. M. Wang, Y. Cheng, and Y. Xiang, "Mechanical properties of bilayer graphene sheets coupled by sp^3 bonding," *Carbon*, vol. 49, pp. 4511–4517, 2011, doi: 10.1016/j.carbon.2011.06.058.

[8] J. S. Bunch, S. S. Verbridge, J. S. Alden, A. M. van der Zande, J. M. Parpia, H. G. Craighead, and P. L. McEuen, "Impermeable atomic membranes from graphene sheets," *Nano Letters*, vol. 8, pp. 2458–2462, 2008, doi: 10.1021/nl801457b.

[9] K. Kanetani, K. Sugawara, T. Sato, R. Shimizu, K. Iwaya, T. Hitosugi, and T. Takahashi, "Ca-intercalated bilayer graphene as the thinnest limit of superconducting C_6Ca," *Proceedings of the National Academy of Sciences*, vol. 109, pp. 19610–19613, 2012, doi: 10.1073/pnas.1208889109.
[10] D. W. Boukhvalov and M. I. Katsnelson, "Tuning the gap in bilayer graphene using chemical functionalization: Density functional calculations," *Physical Review B*, vol. 78, Art. no. 085413, 2008, doi: 10.1103/PhysRevB.78.085413.
[11] C. F. Destefani, S. E. Ulloa, and G. E. Marques, "Spin-orbit coupling and intrinsic spin mixing in quantum dots," *Physical Review B*, vol. 69, Art. no. 125302, 2004, doi: 10.1103/PhysRevB.69.125302.
[12] Q. F. Sun and X. C. Xie, "Bias-controllable intrinsic spin polarization in a quantum dot: Proposed scheme based on spin-orbit interaction," *Physical Review B*, vol. 73, Art. no. 235301, 2006, doi: 10.1103/PhysRevB.73.235301.
[13] A. Kormányos, V. Zólyomi, N. D. Drummond, and G. Burkard, "Spin–orbit coupling, quantum dots, and qubits in monolayer transition metal dichalcogenides," *Physical Review X*, vol. 4, Art. no. 011034, 2014, doi: 10.1103/PhysRevX.4.011034.
[14] A. H. MacDonald, "Bilayer graphene's wicked, twisted road," *Physics*, vol. 12, 2019, doi: 10.1103/Physics.12.12.
[15] H. H. Fu, D. D. Wu, L. Gu, M. H. Wu, and R. Q. Wu, "Design for a spin-Seebeck diode based on two-dimensional materials," *Physical Review B*, vol. 92, Art. no. 045418, 2015, doi: 10.1103/PhysRevB.92.045418.
[16] S. Park, N. Nagaosa, and B. J. Yang, "Thermal Hall effect, spin Nernst effect, and spin density induced by thermal gradient in collinear ferrimagnets from magnon–phonon interaction," *Nano Letters*, vol. 20, pp. 2741–2746, 2020, doi: 10.1021/acs.nanolett.9b05276.
[17] G. M. Choi, C. H. Moon, B. C. Min, K. J. Lee, and D. G. Cahill, "Thermal spin-transfer torque driven by the spin-dependent Seebeck effect in metallic spin valves," *Nature Physics*, vol. 11, pp. 576–581, 2015, doi: 10.1038/nphys3355.
[18] J. Pan *et al*., "Topological valley transport in bilayer graphene induced by interlayer sliding," *Physical Review Letters*, vol. 135, Art. no. 126603, 2025, doi: 10.1103/PhysRevLett.135.126603.
[19] Z. Zhang, J. Dong, H. Hu, Y. Guo, and H. Liu, "Temperature-gradient-controlled spin current rectification in a semiconductor quantum dot," *Journal of Applied Physics*, vol. 137, Art. no. 193902, 2025, doi: 10.1063/5.0266579.
[20] D. Prete *et al*., "Thermoelectric conversion at 30 K in InAs/InP nanowire quantum dots," *Nano Letters*, vol. 19, pp. 3033–3039, 2019, doi: 10.1021/acs.nanolett.9b00442.
[21] Y. L. Feng, Z. L. Wang, X. Zuo, and G. Y. Gao, "Electronic phase transition, spin filtering effect, and spin Seebeck effect in 2D high-spin-polarized VSi_2X_4 (X = N, P, As)," *Applied Physics Letters*, vol. 120, Art. no. 092405, 2022, doi: 10.1063/5.0086990.
[22] P. W. Anderson, "Localized magnetic states in metals," *Physical Review*, vol. 124, no. 1, pp. 41–53, 1961, doi: 10.1103/PhysRev.124.41.
[23] D. M. Newns, "Self-consistent model of hydrogen chemisorption," *Physical Review*, vol. 178, pp. 1123–1135, 1969, doi: 10.1103/PhysRev.178.1123.
[24] T. B. Grimley, "The indirect interaction between atoms or molecules adsorbed on metals," *Proceedings of the Physical Society*, vol. 90, no. 3, pp. 751–760, 1967, doi: 10.1088/0370-1328/90/3/320.
[25] J. W. Gadzuk, J. K. Hartman, and T. N. Rhodin, "Approach to alkali-metal chemisorption within the Anderson model," *Physical Review B*, vol. 4, pp. 241–249, 1971, doi: 10.1103/PhysRevB.4.241.

[26] A. R. Al-Ebady, J. M. Al-Mukh, and S. I. Easa, “Theoretical study of the chemisorption of alkali atoms on graphene sheets,” *Basrah Journal of Science*, vol. 36, pp. 29–44, 2018, doi: 10.29072/basjs.2018104.
[27] A. R. Ahmed, “The electric field effect on the chemisorption of Cu atoms on perfect graphene,” *Basrah Journal of Science*, vol. 41, pp. 96–107, 2023.
[28] G. S. Kliros, “A phenomenological model for the quantum capacitance of monolayer and bilayer graphene devices,” *Romanian Journal of Information Science and Technology*, vol. 13, pp. 332–341, 2010, doi: 10.48550/arXiv.1105.5827.

Journal of Basrah Researches (Sciences) **51**(2), 284 (2025)
DOI: https://doi.org/10.56714/bjrs.51.2.20

الالتصاق الكيميائي لذرتي الليثيوم والصوديوم على الكرافين ثنائي الطبقة

بتول مجيد عجير، اباذر رحمن احمد*

قسم الفيزياء ، كلية التربية للعلوم الصرفة ، جامعة البصرة ، البصرة ، العراق

معلومات البحث

الاستلام 21 تشرين أول 2025
المراجعة 13كانون أول 2025
القبول 22 كانون أول 2025
النشر 31 كانون أول 2025

الكلمات المفتاحية

كرافين ثنائي الطبقة، التصاق كيميائي، نموذج اندرسون-نيونز

الملخص

تم استخدام انموذج اندرسون نيونز لدراسة عملية الالتصاق الكيميائي لذرتي الليثيوم والصوديوم على سطح الكرافين ثنائي الطبقة ، استخدمت كثافة حالات الكرافين ثنائي الطبقة وتأثيرات الاقتران الكمي المتمثلة بالتعريض والازاحة الكمية لحساب الخواص الالكترونية، التمغنط وطاقة الالتصاق الكيميائي. اظهرت الحلول التوافقية الذاتية لأعداد اشغال الذرتين بأن الحل يكون مغناطيسيا للمسافات البعيدة نسبيا عن سطح الكرافين ثنائي الطبقة وعند مسافة معينة من السطح يتحول الى حل غير مغناطيسي , إن علاقة تمغنط الذرات بالمسافة من مستوي الطبقة الثنائية يمكن أن تستثمر في تطبيقات الالكترونيات البرمية. كذلك ان الجزء الايوني من طاقة الالتصاق الكيميائي يكون هو السائد عند اقرب مسافة والذي يعطي الوصف الواضح لنوع التآصر مع الكرافين ثنائي الطبقة. يمكن الاستفادة من هذه النتائج في التطبيقات العملية لتخزين الذرات ذات التمغنط الصفري على المواد ثنائية الأبعاد.

Citation: B. M. Ajer , A. R. Ahmed. , J. Basrah Res. (Sci.) **50**(2), 284 (2025). DOI:https://doi.org/10.56714/bjrs.51.2.20

***Corresponding author email:** abadhar.ahmed@uobasrah.edu.iq.

ISSN: 1817-2695 (Print); 2411-524X (Online)
Online at: https://jou.jobrs.edu.iq